# UCLA
## UCLA Previously Published Works

**Title**

Photoelectron spectroscopic and computational study of the PtMgH 3,5 − cluster anions

**Permalink**

**Journal**

**ISSN**

**Authors**

Zhang, Xinxing
Ganteför, Gerd
Alexandrova, Anastassia N
et al.

**Publication Date**

**DOI**

Peer reviewed

# PAPER

# Photoelectron spectroscopic and computational study of the PtMgH$_{3,5}^{-}$ cluster anions†

Xinxing Zhang,[a] Gerd Ganteför,[a] Anastassia N. Alexandrova[bc] and Kit Bowen*[a]

The two cluster anions, PtMgH$_3^-$ and PtMgH$_5^-$, were studied by photoelectron spectroscopy and theoretical calculations. Experimentally-determined electron affinity (EA) and vertical detachment energy (VDE) values were compared with those predicted by our computations; excellent agreement was found. The calculated structures of PtMgH$_3^-$ and PtMgH$_3$ both exhibit $\eta_2$-bonded H$_2$ moieties. Activation of these H$_2$ moieties is implied by the elongation of their bond lengths relative to the bond length of free H$_2$. The calculated structures of PtMgH$_5^-$ and PtMgH$_5$ both exhibit all-hydrogen, five-member, $\sigma$-aromatic rings. These attributes are responsible for this anion's special stability.

## Introduction

The interaction between hydrogen and small bimetallic clusters containing precious metal elements has gathered considerable attention in catalysis, *e.g.*, in hydrogenation and dehydrogenation reactions.[1–7] Doping commonly used hydrogenation or dehydrogenation catalysts, such as Ni, Pd, Pt, with another metal has been found to be beneficial in fine-tuning catalytic activity, *e.g.*, by lowering the H–H bond activation barrier.[2] Nevertheless, studies exploring the reasons for why mixed metal catalysts are better than single metal ones are scarce. It has been suggested that doping can tune the electronic structure by adjusting the position of the d-band center.[8] A theoretical study on H$_2$ dissociation by doped Ni clusters showed that dopants such as Rh, Pd, Pt, and Au could lower the H$_2$ activation barrier.[2] A density functional theory study observed that the adsorption of H$_2$ on Au$_n$Cu$_m$ clusters enhanced the stability of the whole cluster.[4] A comparative study of CH$_3$OH dehydrogenation on Pt$_7$ *versus* Pt$_5$Ni$_2$ found that charge transfer from Ni to Pt increased the electron density on the platinum atoms' 5d orbital, thereby improving the catalytic activity of the Pt$_5$Ni$_2$ cluster relative to Pt$_7$.[5] More recently, we reported that the mixed metal hydride cluster anion, PtZnH$_5^-$, has a planar five-coordinated structure and unusual stability owing to its $\sigma$-aromaticity.[1]

Here, we extend our study of mixed metal hydride cluster anions to PtMgH$_3^-$ and PtMgH$_5^-$, characterizing them using a combination of anion photoelectron spectroscopy and theoretical calculations. The geometric and electronic structures of these two systems revealed unique chemical bonding features between their hydrogen atoms and their metal centers.

## Experimental and theoretical methods

This work utilized anion photoelectron spectroscopy as its primary experimental probe. Anion PES is conducted by crossing a mass-selected beam of negative ions with a fixed-energy photon beam and energy analyzing the resulting photodetached electrons. This technique is governed by the energy conservation relationship, $h\nu$ = EBE + EKE, where $h\nu$, EBE, and EKE are the photon energy, electron binding (transition) energy, and the electron kinetic energy, respectively. Our photoelectron spectrometer, which has been described earlier, consists of one of several ion sources, a linear time-of-flight mass spectrometer, a mass gate, a momentum decelerator, a neodymium-doped yttrium aluminum garnet (Nd:YAG) laser for photodetachment, and a magnetic bottle electron energy analyzer, having a resolution of 35 meV at EKE = 1 eV.[9] Photoelectron spectra were calibrated against the well-known photoelectron spectrum of Cu$^-$.[10] PtMgH$_{3,5}^-$ anions were generated using a pulsed arc cluster ionization source (PACIS), which has been described in detail elsewhere.[11] This source has proven to be a powerful tool for generation metal and metal hydride cluster anions.[11–22] Briefly, a $\sim$30 μs long 150 V electrical pulse, applied across the anode and sample cathode of the discharge chamber, vaporized Pt and Mg atoms, the sample cathode having been prepared in a glove box by pressing Mg and Pt powders onto a copper rod. Almost simultaneously, 200 psi of ultrahigh purity hydrogen gas was injected into the discharge region, where it dissociated into hydrogen atoms. The resulting mixture of atoms, ions, and electrons then reacted and cooled as it flowed along a 15 cm

*a Department of Chemistry, Johns Hopkins University, Baltimore, Maryland 21218, USA. E-mail: kbowen@jhu.edu; Tel: +1-410-516-8425*

*b Department of Chemistry and Biochemistry, University of California, Los Angeles, Los Angeles, California, 90095, USA*

*c California NanoSystems Institute, 570 Westwood Plaza, Building 114, Los Angeles, CA 90095, USA*

† Electronic supplementary information (ESI) available. See DOI: 10.1039/c6cp03243e

This journal is © the Owner Societies 2016

*Phys. Chem. Chem. Phys.*, 2016, **18**, 19345–19349 | 19345

**Paper**

tube before exiting into high vacuum. The resulting anions were then extracted and mass-selected prior to photodetachment.

Density functional theory calculations were conducted by applying PBEPBE functional[23] using the Gaussian09 software
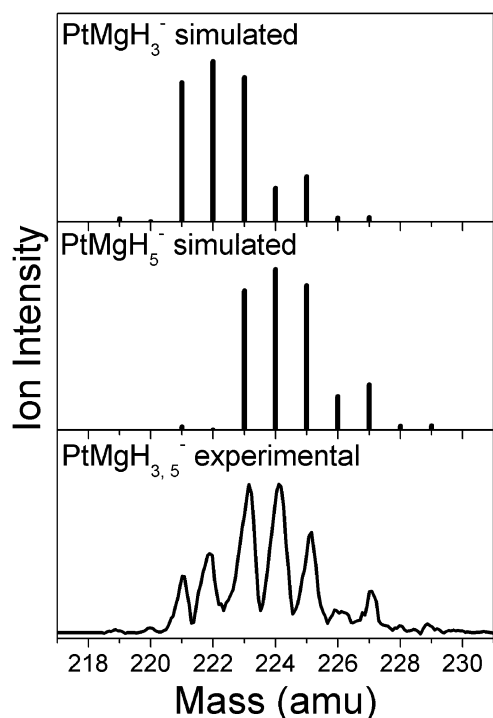
package[24] to determine the geometries of both neutral and anionic clusters, the electron affinity (EA) and vertical detachment energy (VDE) values, and the charge distribution. All geometries, including that of the anion and its corresponding neutral molecule, were fully optimized without any geometrical constraints using the 6-311++G (3df, 3pd) basis set[25] for Mg and H, and the LANL2DZ effective core potentials for Pt.[26–28] The EA value is the energy difference between the ground state of the neutral and the ground state of the anion with zero point energy correction having been applied. The VDE is the energy difference between the ground state of the anion and the neutral, having the same structure as the anion. Natural population analysis (NPA), as implemented in the Gaussian09 code, was also carried out to determine the charge distribution of the anions. The NPA method has been found to be satisfactory in calculating the charge distribution within clusters.[29]

## Results and discussion

Fig. 1 presents the simulated and experimental mass spectral distributions of $PtMgH_3^-$ and $PtMgH_5^-$. One observes that $PtMgH_3^-$ and $PtMgH_5^-$ coexist in the ion beam. To avoid mass



**Fig. 1** Simulated and experimental isotopic (mass) distributions for $PtMgH_3^-$ and $PtMgH_5^-$.

**Table 1** Experimental and theoretical EA values for $PtMgH_{3,5}$ as well as experimental and theoretical VDE values for $PtMgH_{3,5}^-$. All values are in eV

| System | Expt. EA | Theo. EA | Expt. VDE | Theo. VDE |
|---|---|---|---|---|
| $PtMgH_3^{-/0}$ | 1.45 | 1.48 | 1.80 | 1.73 |
| $PtMgH_5^{-/0}$ | 1.85 | 1.93 | 2.05 | 2.03 |
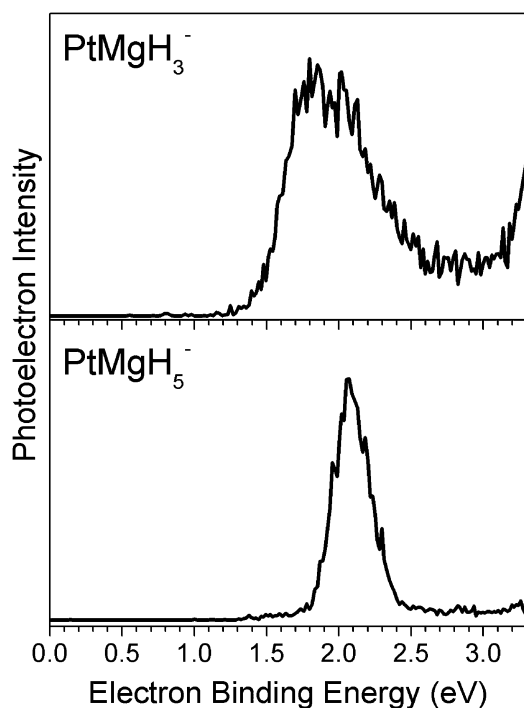


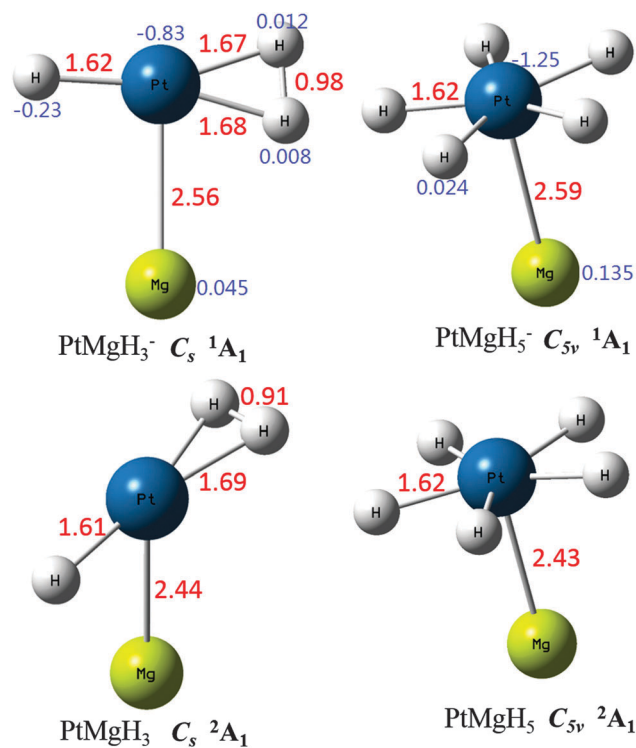**Fig. 2** Photoelectron spectra of $PtMgH_3^-$ and $PtMgH_5^-$, both recorded with 3.490 eV photons.



**Fig. 3** Calculated structures of $PtMgH_{3,5}^{-/0}$. The bond lengths (Å) are shown in red and the charge distributions (e) in blue. The point group and electronic state of each cluster are also presented.

overlaps, the photoelectron spectrum of $PtMgH_3^-$ was recorded at mass = 221 and 222, while the photoelectron spectrum of $PtMgH_5^-$ was measured at mass = 226 and 227. By taking photoelectron spectra at all masses in this mass window and carefully comparing them, we confirmed that no other $PtMgH_n^-$ cluster anions were in the beam. $PtMgH_3^-$ and $PtMgH_5^-$ dominate, over other possible $PtMgH_n^-$ cluster anion stoichiometries, because of their high stabilities. Moreover, the ion intensity of $PtMgH_5^-$ is higher than that of $PtMgH_3^-$, suggesting that $PtMgH_5^-$ may be the stabilizer of the two.

The photoelectron spectra of $PtMgH_3^-$ and $PtMgH_5^-$ are shown in Fig. 2. For $PtMgH_3^-$, one observes a broad EBE band that begins at EBE = 1.45 eV and reaches its maximum at EBE = 1.80 eV. For $PtMgH_5^-$, its single band begins at EBE = 1.85 eV and reaches its maximum at EBE = 2.05 eV. The photoelectron band for $PtMgH_5^-$ is significantly narrower than that for $PtMgH_3^-$. This suggests that the geometric structures of $PtMgH_5^-$ and $PtMgH_5$ are relatively similar to one another, whereas the geometric structures of $PtMgH_3^-$ and $PtMgH_3$ are less so. Moreover, similar
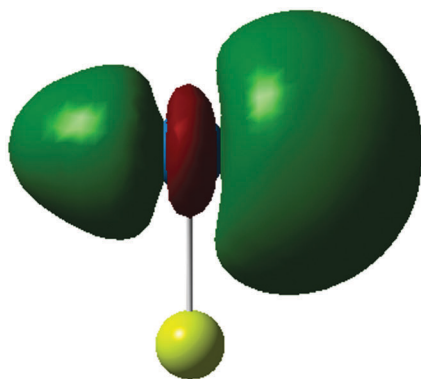


Fig. 4 The MO of $PtMgH_3^-$, highlighting that of the $Pt(\eta_2\text{-}H_2)$ bond.

structures lead to good Franck–Condon overlap. When there is good Franck–Condon overlap between the ground state of the anion and the ground state of its neutral counterpart, and when the vibrationally excited states of the anion are poorly populated (when no significant hot bands are in evidence), the photoelectron signal threshold of the lowest EBE band should be close to the electron affinity (EA) of the anion's neutral counterpart. The EBE values of the band maxima, mentioned above, correspond to the anions' vertical detachment energies (VDE). Both the experimental and the computational EA and VDE values for $PtMgH_3$ and $PtMgH_3^-$, respectively and for $PtMgH_5$ and $PtMgH_5^-$, respectively are tabulated in Table 1. One sees that the agreement is quite good.

Fig. 3 presents the calculated geometric structures of $PtMgH_3$ and $PtMgH_3^-$ and of $PtMgH_5$ and $PtMgH_5^-$. The bond lengths (Å) are marked with red numbers. $PtMgH_3^-$ ($^1A_1$) has a planar $C_s$ structure, in which the H–H moiety is bound to the Pt atom. The bond length between these two associated H atoms is 0.98 Å. This is significantly longer than the bond length in the free $H_2$ molecule (0.74 Å), indicating that the $H_2$ moiety in $PtMgH_3^-$ is highly activated. Neutral $PtMgH_3$ ($^2A_1$) has a 3-D $C_s$ structure, where the H–Pt–Mg plane perpendicularly bisects the H–H bond. $PtMgH_5^-$ ($^1A_1$), on the other hand, has a $C_{5v}$ umbrella-like structure, where all the H atoms are bonded to the Pt atom, forming an all-hydrogen, five-member ring. Platinum is often found to be tetra-coordinated and square planar. Here in $PtMgH_5^-$, however, we see a five-coordinated arrangement of H atoms in-plane and a Mg atom at the axial position. Such a structure is very similar to our previously reported $PtZnH_5^-$ cluster[1] as well as to other examples seen in theoretical calculations.[30] Neutral $PtMgH_5$ ($^2A_1$), which also exhibits $C_{5v}$ symmetry, is very similar to the $PtZnH_5^-$ anion, the main difference being its shorter Pt–Mg bond. The coordinates of all of these structures are reported in the ESI.†
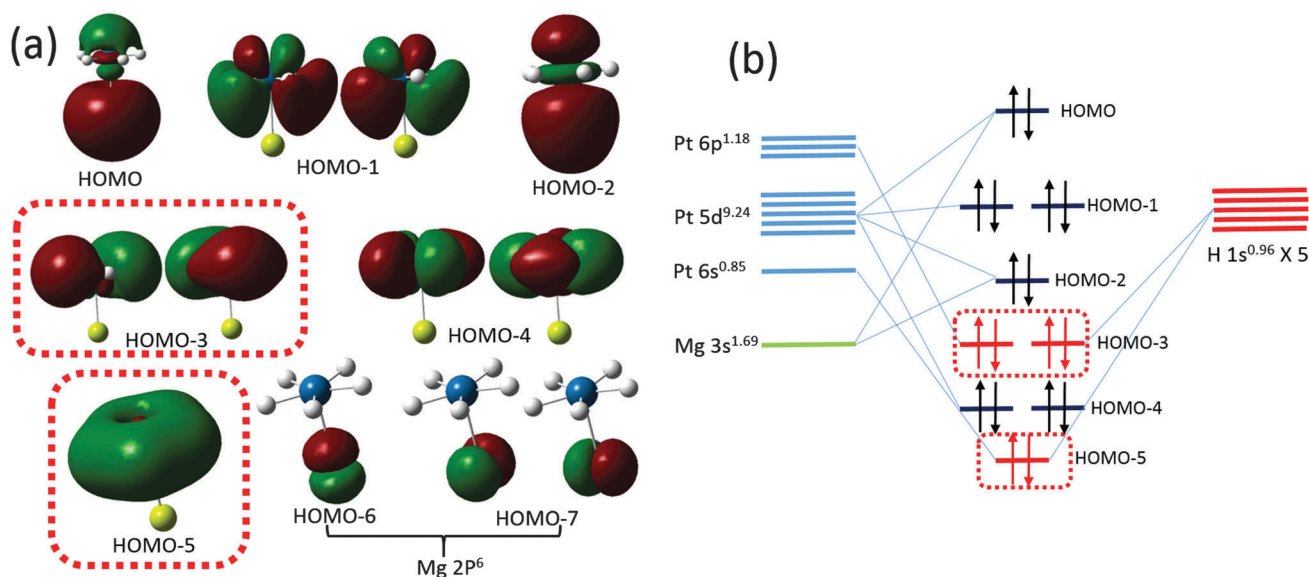


Fig. 5 Chemical bonding in $PtMgH_5^-$. (a) Valence MO's, with the ones outlined in red corresponding to the σ-aromatic MO's. (b) Correlation diagram for the valence MO's.

The charge distribution on each atom in both cluster anions was obtained from natural population analysis, and these are marked in blue in Fig. 3. In $PtMgH_3^-$, the Pt atom draws most of the negative charge, due to its relatively high electronegativity. While the radially bonded H atom has a negative charge of $-0.23\ e$, the H atoms of the H–H moiety are almost neutral, reflecting the fact that the H–H moiety is a $H_2$ molecule, albeit an activated one. Thus, the $PtMgH_3^-$ cluster can be viewed as an activated $\eta_2$-$H_2$ molecule attached to a $PtMgH^-$ moiety. Clusters exhibiting $\eta_2$-bonded $H_2$ have been seen in $M(CO_3)(Pr_3)_2(H_2)$,[31] in $(\eta^2$-$H_2)CuCl$ clusters in argon matrices,[32] in gas-phase $[HPd(\eta^2$-$H_2)]^-$ species,[18] and in both $(\eta^2$-$H_2)CuF$ and $(\eta^2$-$H_2)AgCl$ neutral clusters.[33,34] In each of these cases, $H_2$ was bound to the rest of the molecule or cluster by a significant binding energy.

Fig. 4 shows the two-electron, three-center (2e3c) molecular orbital of the $Pt(\eta_2$-$H_2)$ bond, overlaid on the $PtMgH_3^-$ framework. This orbital is very similar to the corresponding molecular orbital in $(\eta_2$-$H_2)CuCl$.[32] Note that the charge on the Mg atom is almost neutral (see Fig. 3), showing that the Mg atom can be viewed as a spectator in the system. Since the non-magnesium part of the cluster, i.e., $[HPt(\eta_2$-$H_2)]^-$, is isovalent to $(\eta_2$-$H_2)CuCl$[32] and to $[HPd(\eta^2$-$H_2)]^-$,[18] it is not surprising that similar chemical bonding should be observed. The energy required to dissociate $\eta_2$-bonded $H_2$ from $PtMgH_3^-$ was calculated as $E(PtMgH^-) + E(H_2) - E(PtMgH_3^-)$. The resulting dissociation energy is 101 kJ mol$^{-1}$, showing that the $H_2$'s binding is quite strong. This value is comparable to those for other $\eta_2$-bonded $H_2$ clusters (80–110 kJ mol$^{-1}$).[18,31–34]

Next, we discuss the chemical bonding in $PtMgH_5^-$. Again, due to its relatively high electronegativity, Pt in $PtMgH_5^-$ is negatively charged by $-1.25\ e$ (Fig. 3). Fig. 5(a) presents the valence molecular orbitals (MO's) of $PtMgH_5^-$, with the ones outlined in red corresponding to the σ-aromatic MO's. Fig. 5(b) shows how the MO's are formed from the combination of atomic orbitals, with those highlighted in red corresponding to the σ-aromatic MO's in Fig. 5(a). It appears that HOMO−1 and HOMO−4 are the d lone pairs of Pt, while HOMO−6 and HOMO−7 are the p orbitals of Mg. HOMO and HOMO−2 correspond to the σ bond between Pt and Mg. These MO's are the bonding and anti-bonding combinations of the $5d_{z^2}$ atomic orbital of Pt and 3s atomic orbital of Mg. The most interesting MO's are the HOMO−5 and the doubly degenerate HOMO−3; they are the σ-aromatic objects. These orbitals are formed from the combination of the five 1s atomic orbitals of the five H atoms and 6p and 6s atomic orbitals of Pt. The electronic configuration of Pt is $5d^9 6s^1$, but in this $PtMgH_5^-$ cluster, Pt has a $5d^{9.25} 6s^{0.85} 6p^{1.18}$ electronic configuration, consistent with the fact that Pt is negatively charged by $-1.25\ e$, hence, Pt acts as an electron donor of the $H_5$ ring, making it an $H_5^-$ moiety. Occupied by a total of six electrons, the HOMO−3 and HOMO−5 together are the basis for its σ-aromaticity,[35,36] fulfilling the $4n + 2$ Hückel rule, where $n = 1$. It is this special σ-aromaticity that makes $PtMgH_5^-$ an unusually stable cluster anion and explains its high abundance in the mass spectrum.

Lastly, $PtMgH_5^-$ and previously studied $PtZnH_5^-$ have much in common.[1] Since both Mg and Zn have two valence electrons, $PtMgH_5^-$ and $PtZnH_5^-$ exhibit similar structural and bonding features. Both can also be described as systems in which Pt and an $H_5$ pentagon are coordinated, and they can be written as $[MgPt(\eta_5$-$H_5)]^-$ and $[ZnPt(\eta_5$-$H_5)]^-$. Mixed-metal hydride clusters such as these may have roles to play as hydrogenation catalysts.

## Acknowledgements

## References

1  X. Zhang, G. Liu, G. Gantefoer, K. H. Bowen and A. N. Alexandrova, *J. Phys. Chem. Lett.*, 2014, **5**, 1596.
2  N. S. Venkataramanan, A. Suvitha, H. Mizuseki and Y. Kawazoe, *Int. J. Quantum Chem.*, 2013, **113**, 1940.
3  L. B. Ortiz-Soto, J. R. Monnier and M. D. Amiridis, *Catal. Lett.*, 2006, **107**, 13.
4  S. Zhao, X. Tian, J. Liu, Y. Ren, Y. Ren and J. Wang, *J. Cluster Sci.*, 2015, **26**, 491.
5  W. Guo, W. Tian, X. Lian, F. Liu, M. Zhou, P. Xiao and Y. Zhang, *Comput. Theor. Chem.*, 2014, **1032**, 73.
6  H. Liu, *Quantum Matter*, 2014, **3**, 119.
7  X. Zhang, G. Gantefoer, K. H. Bowen and A. Alexandrova, *J. Chem. Phys.*, 2014, **140**, 164316.
8  J. Rossmeisl, G. S. Karlberg, T. Jaramillo and J. K. Norskov, *Faraday Discuss.*, 2009, **140**, 337.
9  M. Gerhards, O. C. Thomas, J. M. Nilles, W. J. Zheng and K. H. Bowen, *J. Chem. Phys.*, 2002, **116**, 10247.
10 J. Ho, K. M. Ervin and W. C. Lineberger, *J. Chem. Phys.*, 1990, **93**, 6987.
11 X. Zhang, Y. Wang, H. Wang, A. Lim, G. Ganteför, K. H. Bowen, J. U. Reveles and S. N. Khanna, *J. Am. Chem. Soc.*, 2013, **135**, 4856.
12 A. S. Ivanov, X. Zhang, H. Wang, A. I. Boldyrev, G. Gantefoer, K. H. Bowen and I. Černušák, *J. Phys. Chem. A*, 2015, **119**, 11293.
13 J. Joseph, K. Pradhan, P. Jena, H. Wang, X. Zhang, Y. J. Ko and K. H. Bowen, *J. Chem. Phys.*, 2012, **136**, 194305.
14 X. Zhang, B. Visser, M. Tschurl, E. Collins, Y. Wang, Q. Wang, Y. Li, Q. Sun, P. Jena, G. Gantefoer, U. Boesl, U. Heiz and K. H. Bowen, *J. Chem. Phys.*, 2013, **139**, 111101.
15 A. Buytendyk, J. Graham, H. Wang, X. Zhang, E. Collins, Y. J. Ko, G. Gantefoer, B. Eichhorn, A. Regmi, K. Boggavarapu and K. H. Bowen, *Int. J. Mass Spectrom.*, 2014, **365**, 140.
16 H. Wang, X. Zhang, J. Ko, A. Grubisic, X. Li, G. Ganteför, H. Schnöckel, B. Eichhorn, M. Lee, P. Jena, A. Kandalam, B. Kiran and K. H. Bowen, *J. Chem. Phys.*, 2014, **140**, 054301.
17 H. Wang, Y. Ko, X. Zhang, G. Gantefoer, H. Schnoeckel, B. W. Eichhorn, P. Jena, B. Kiran, A. K. Kandalam and K. H. Bowen, *J. Chem. Phys.*, 2014, **140**, 124309.
18 X. Zhang, P. Robinson, G. Gantefoer, A. Alexandrova and K. H. Bowen, *J. Chem. Phys.*, 2015, **143**, 094307.

19 H. Wang, X. Zhang, Y. Ko, G. F. Ganteför, K. H. Bowen, X. Li, K. Boggavarapu and A. Kandalam, *J. Chem. Phys.*, 2014, **140**, 164317.

20 X. Zhang, H. Wang, E. Collins, A. Lim, G. Ganteför, B. Kiran, H. Schnöckel, B. Eichhorn and K. H. Bowen, *J. Chem. Phys.*, 2013, **138**, 124303.

21 J. D. Graham, A. M. Buytendyk, X. Zhang, E. L. Collins, K. Boggavarapu, G. Gantefoer, B. W. Eichhorn, G. L. Gutsev, S. Behera, P. Jena and K. H. Bowen, *J. Phys. Chem. A*, 2014, **118**, 8158.

22 X. Zhang, H. Wang, G. Ganterför, B. Eichhorn and K. Bowen, *Int. J. Mass Spectrom.*, 2016, **404**, 24.

23 J. P. Perdew, K. Burke and M. Ernzerhof, *Phys. Rev. Lett.*, 1996, **77**, 3865.

24 M. J. Risch, G. W. Trucks, H. B. Schlegel, G. E. Scuseria, M. A. Robb, J. R. Cheeseman, G. Scalmani, V. Barone, B. Mennucci and G. A. Petersson, *et al.*, *Gaussian 09, revision A.1*, Gaussian, Inc., Wallingford, CT, 2009.

25 R. Krishnan, J. S. Binkley, R. Seeger and J. A. Pople, *J. Chem. Phys.*, 1980, **72**, 650.

26 P. J. Hay and W. R. Wadt, *J. Chem. Phys.*, 1985, **82**, 270.

27 P. J. Hay and W. R. Wadt, *J. Chem. Phys.*, 1985, **82**, 284.

28 P. J. Hay and W. R. Wadt, *J. Chem. Phys.*, 1985, **82**, 299.

29 I. A. Popov, X. Zhang, B. W. Eichhorn, A. Boldyrev and K. H. Bowen, *Phys. Chem. Chem. Phys.*, 2015, **17**, 26079.

30 E. Jimenez-Izala and A. N. Alexandrova, *Phys. Chem. Chem. Phys.*, 2016, **18**, 11644.

31 G. J. Kubas, R. R. Ryan, B. I. Swanson, P. J. Vergamini and H. J. Wasserman, *J. Am. Chem. Soc.*, 1984, **106**, 452.

32 H. S. Von Plitt, M. R. Bar, R. Ahlrichs and H. Schnockel, *Angew. Chem.*, 1991, **103**, 848.

33 G. S. Grubbs II, D. A. Obenchain, H. M. Pickett and S. E. Novick, *J. Chem. Phys.*, 2014, **141**, 114306.

34 D. J. Frohman, G. S. Grubbs, II, Z. Yu and S. E. Novick, *Inorg. Chem.*, 2013, **52**, 816.

35 A. N. Alexandrova, A. I. Boldyrev, X. Li, H. W. Sarkas, J. H. Hendricks, S. T. Arnold and K. H. Bowen, *J. Chem. Phys.*, 2011, **134**, 044322.

36 A. N. Alexandrova and A. I. Boldyrev, *J. Phys. Chem. A*, 2003, **107**, 554.

This journal is © the Owner Societies 2016

*Phys. Chem. Chem. Phys.*, 2016, **18**, 19345–19349 | **19349**